

## ARTICLE

# Recommendations for the Design of Clinical Drug–Drug Interaction Studies With Itraconazole Using a Mechanistic Physiologically-Based Pharmacokinetic Model

Yuan Chen<sup>1,\*</sup>, Tamara D. Cabalu<sup>2</sup>, Ernesto Callegari<sup>3</sup>, Heidi Einolf<sup>4</sup>, Lichuan Liu<sup>5</sup>, Neil Parrott<sup>6</sup>, Sheila Annie Peters<sup>7</sup> , Edgar Schuck<sup>8</sup>, Pradeep Sharma<sup>9</sup>, Helen Tracey<sup>10</sup>, Vijay V. Upreti<sup>11</sup>, Ming Zheng<sup>12</sup>, Andy Z.X. Zhu<sup>13</sup> and Stephen D. Hall<sup>14</sup>

Regulatory agencies currently recommend itraconazole (ITZ) as a strong cytochrome P450 3A (CYP3A) inhibitor for clinical drug–drug interaction (DDI) studies. This work by an International Consortium for Innovation and Quality in Pharmaceutical Development working group (WG) is to develop and verify a mechanistic ITZ physiologically-based pharmacokinetic model and provide recommendations for optimal DDI study design based on model simulations. To support model development and verification, *in vitro* and clinical PK data for ITZ and its metabolites were collected from WG member companies. The model predictions of ITZ DDIs with seven different CYP3A substrates were within the guest criteria for 92% of area under the concentration–time curve ratios and 95% of maximum plasma concentration ratios, thus verifying the model for DDI predictions. The verified model was used to simulate various clinical DDI study scenarios considering formulation, duration of dosing, dose regimen, and food status to recommend the optimal design for maximal inhibitory effect by ITZ.

## Study Highlights

### WHAT IS THE CURRENT KNOWLEDGE ON THE TOPIC?

☑ Recommendations for the design of itraconazole (ITZ) drug–drug interaction (DDI) studies are currently based on the literature review of clinical data, and the existing ITZ physiologically-based pharmacokinetic (PBPK) models were either developed using a top-down approach or developed with an insufficient mechanistic understanding.

### WHAT QUESTION DID THIS STUDY ADDRESS?

☑ This study addresses whether it is feasible to build a PBPK model with a better mechanistic understanding to predict pharmacokinetics (PK) and DDIs with increased confidence and subsequently recommend the optimal ITZ DDI study design based on DDI simulations under various scenarios.

### WHAT DOES THIS STUDY ADD TO OUR KNOWLEDGE?

☑ The PBPK model developed in this study describes the PK accumulation of ITZ and hydroxyitraconazole well after repeat dosing of ITZ as a solution and capsule under both fasted and fed states. The model predicted clinical ITZ DDIs with higher confidence; therefore, it can be used to guide clinical DDI study design.

### HOW MIGHT THIS CHANGE DRUG DISCOVERY, DEVELOPMENT, AND/OR THERAPEUTICS?

☑ The study design recommended in this work is based on PBPK simulations and considers formulation, duration of dosing, dose regimen, and food status and largely confirms the design proposed by the Clinical Pharmacology Leadership Group based on the maximal inhibitory effect of ITZ on a new chemical entity in the clinic.

Cytochrome P450 3A (CYP3A) enzymes are often significant contributors to the clearance (CL) of drugs and therefore strong inhibitors that are selective for these enzymes are employed in clinical drug–drug interaction (DDI) studies.

Ketoconazole, a strong, selective, and reversible inhibitor of CYP3A, has been widely employed to determine the maximum drug interaction risk with CYP3A substrates. However, ketoconazole can no longer be used in clinical DDI studies

<sup>1</sup>Department of Drug Metabolism and Pharmacokinetics, Genentech Inc., a member of the Roche Group, South San Francisco, California, USA; <sup>2</sup>Department of Pharmacokinetics, Pharmacodynamics, and Drug Metabolism, Merck & Co., Inc., Kenilworth, New Jersey, USA; <sup>3</sup>Pharmacokinetics, Dynamics and Metabolism, Pfizer Inc., Groton, Connecticut, USA; <sup>4</sup>Modeling & Simulation, PK Sciences, Novartis Institutes for Biomedical Research, East Hanover, New Jersey, USA; <sup>5</sup>Genentech Inc., a member of the Roche Group, South San Francisco, California, USA; <sup>6</sup>Pharmaceutical Sciences, Pharmaceutical Research and Early Development, Roche Innovation Centre, Basel, F. Hoffmann-La Roche Ltd., Basel, Switzerland; <sup>7</sup>Translational Quantitative Pharmacology, Merck KGaA, Darmstadt, Germany; <sup>8</sup>Modeling & Simulation, Clinical Pharmacology Science/Medicine Development Center (MDC), Eisai Inc., Woodcliff Lake, New Jersey, USA; <sup>9</sup>Mechanistic Safety and ADME Sciences, Drug Safety and Metabolism, Innovative Medicines (IMED) Biotech Unit, AstraZeneca R&D, Cambridge, UK; <sup>10</sup>Department of Mechanistic Safety and Disposition, GlaxoSmithKline, Hertfordshire, UK; <sup>11</sup>Clinical Pharmacology Modeling and Simulation, Amgen Inc., South San Francisco, California, USA; <sup>12</sup>Clinical Pharmacology and Pharmacometrics, Bristol-Myers Squibb Company, Princeton, New Jersey, USA; <sup>13</sup>Department of Drug Metabolism and Pharmacokinetics, Takeda Pharmaceuticals International Co., Cambridge, Massachusetts, USA; <sup>14</sup>Lilly Research Laboratories, Eli Lilly and Company, Indianapolis, Indiana, USA. \*Correspondence: Yuan Chen ([chen.yuan@gene.com](mailto:chen.yuan@gene.com))

Received: February 5, 2019; accepted: June 11, 2019. doi:10.1002/psp4.12449

because of concerns regarding hepatotoxicity highlighted by the European Medicines Agency<sup>1</sup> and the US Food and Drug Administration.<sup>2</sup> Based on a literature review, the Innovation and Quality in Pharmaceutical Development's (IQ) Clinical Pharmacology Leadership Group (CPLG) provided recommendations for best practices when using itraconazole (ITZ) in clinical DDI studies.<sup>3</sup> However, as pointed out in the CPLG recommendations, the impact of multiple factors on the extent of DDI, such as the choice of ITZ dosage form, food status, dosing, and duration of ITZ administration as well as the timing of substrate and ITZ co-administration should be further examined and physiologically-based pharmacokinetic (PBPK) modeling may play an important role in ITZ DDI study design.

Developing a mechanistic PBPK ITZ model is challenging because of the complexity of the pharmacokinetics (PK) and the extreme physicochemical properties of ITZ and its metabolites. Following ITZ administration, CYP3A enzymes, both in the gut wall and the liver, are reversibly inhibited by the parent drug and potentially by the sequentially formed metabolites, hydroxyitraconazole (OH-ITZ), keto-itraconazole (keto-ITZ), and N-desmethylitraconazole (ND-ITZ). The formation of these inhibitory metabolites is catalyzed by CYP3A4, which leads to nonlinear PK. The characterization of these inhibitory species *in vitro* is challenging because of their high lipophilicity and low aqueous solubility, and this has resulted in a wide range of reported values for the fraction unbound in plasma ( $f_{u,p}$ ) and liver microsomal preparations ( $f_{u,mic}$ ). Although ITZ PBPK models have been previously developed,<sup>4,5</sup> these were built using a "top-down" approach because of the uncertainty in the *in vitro* data required for model construction. More recently published<sup>6,7</sup> mechanistic models demonstrated acceptable DDI simulation results, but the general applicability is uncertain

because of the key *in vitro* data used, e.g., much larger  $f_{u,p}$  than the experimentally determined values. In addition, the recommendations for the optimal clinical ITZ DDI study design using a PBPK model with a better mechanistic understanding are expected by pharmaceutical companies and regulatory agencies.

The goal of the current study, conducted by this IQ working group (WG) with members from both Drug Metabolism and Clinical Pharmacology Leadership Groups, was to develop an ITZ PBPK model using newly generated data from 12 member companies to address the gaps in currently existing models with respect to key model input parameters in an effort to increase the confidence in DDI simulations and to enable optimal DDI study design and data interpretation. The recommended practices for clinical DDI studies with ITZ are proposed to enable clinical development, including regulatory interactions and prioritization of clinical studies.<sup>8,9</sup>

## METHODS

The model development and verification process is shown in **Figure 1** and detailed in the following sections.

### Data collection

**Clinical PK data.** ITZ PK data from 24 clinical studies were collected for model development and verification (**Table S1**). Clinical data included solution and capsule formulations administered under fasted and fed conditions, representing various PK and DDI study scenarios. Five sets<sup>10–14</sup> of published ITZ clinical PK data were used in model development, and 19 sets of ITZ and OH-ITZ clinical data from the WG were used to assess model performance. Of these 19 studies, 13 were conducted using the SPORANOX solution of ITZ under fasted conditions and 6 using the

### ITZ and OH-ITZ PBPK Model Development and Verification Process

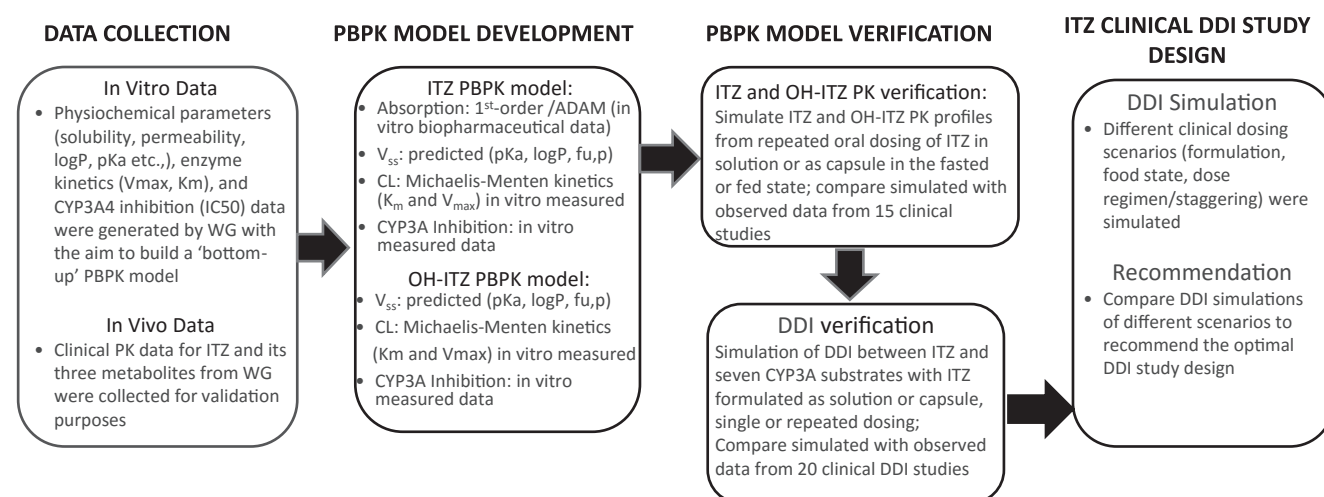


**Figure 1** Itraconazole (ITZ) and hydroxyitraconazole (OH-ITZ) physiologically-based pharmacokinetic (PBPK) model development and verification process. ADAM, advanced dissolution, absorption, and metabolism; CL, clearance; CYP3A, cytochrome P450 3A; DDI, drug–drug interaction;  $f_{u,p}$ , free fraction in plasma;  $k_{in}$ , rate constant from systemic compartment to single adjusting compartment; logP, octanol-water partition coefficient; PK, pharmacokinetics; pKa, acid dissociation constant;  $V_{max}$ , maximum rate of reaction;  $V_{ss}$ , volume of distribution at steady state; WG, working group.

capsule (5 under fed conditions and 1 fasted). Most studies used in the model development and verification had both ITZ and OH-ITZ concentration-time profiles. Six studies collected from WG also had data for keto-ITZ and ND-ITZ.

**Clinical DDI data.** The University of Washington Drug Interaction Database<sup>15</sup> was searched for trials in which the *in vivo* inhibition effect of ITZ was >20%. This list was further narrowed to the following CYP3A4 substrates with a PBPK model available in the Simcyp simulator (Certara UK Limited, Sheffield, UK): midazolam (MDZ), paroxetine, quinidine, repaglinide, simvastatin, triazolam, and zolpidem. Details of the 20 clinical DDI data sets<sup>16–31</sup> are listed in **Table S2**.

**Physicochemical properties and *in vitro* data.** Key physicochemical and *in vitro* data were generated for ITZ and its metabolites by the WG. Descriptions of the methods used are provided in the **Supplementary Material**.

#### PBPK model development

Using the *in vitro* data (CYP3A4 unbound inhibition constant ( $K_{i,u}$ ) and  $f_{u,p}$ ) and clinical PK data collected by the WG, the potential contribution of ITZ and its three circulating metabolites to the *in vivo* DDIs was evaluated by comparing *in vivo* unbound concentrations with *in vitro* unbound  $K_i$  values. The results suggest that significant contributions from keto-ITZ and ND-ITZ to overall inhibition are low; therefore, these metabolites were not included in the model.

A PBPK model was constructed for ITZ and OH-ITZ using the Simcyp Simulator V16 (Certara UK Limited). The model input parameters are shown in **Table 1**. The CL was parameterized with Michaelis–Menten kinetics, and volume of distribution at steady state ( $V_{ss}$ ) for both ITZ and OH-ITZ was predicted from *in vitro* data. The absorption model was built using *in vitro* biopharmaceutical data and refined using clinical data in a mixed “bottom-up” and “top-down” approach. The ability of the model to predict the PK of ITZ and OH-ITZ after single and multiple oral doses of ITZ in either solution or capsule formulation in the fasted and fed states was verified using the clinical data submitted by the WG (**Table S1**). The model's ability to capture DDIs between ITZ and a set of CYP3A4 substrates was verified using published clinical data (**Table S2**).

**PBPK model for ITZ Absorption.** Both oral solution and capsule dosage forms of ITZ are commonly used. Both formulations show a food effect, with the solution giving higher exposure in the fasted state, whereas the capsules give higher exposures with food.<sup>12,13</sup> To maximize the exposures in DDI studies, it has been recommended that the solution be administered in the fasted state. If capsules are preferred, then adequate exposures are achievable if dosed with food.<sup>3</sup> Therefore, even though three absorption models for solution (fasted) and capsule (fasted and fed) were built initially, the model verification was focused on the solution under fasted conditions and the capsule under fed conditions.

Both first-order and advanced dissolution, absorption, and metabolism (ADAM) models were built, and their performance in predicting ITZ and OH-ITZ PK was evaluated. In the first-order absorption model, the fraction absorbed ( $f_a$ ) and rate constant ( $k_a$ ) for ITZ solution (fasted) and capsule (fed and

fasted) were determined using a top-down approach based on previously published clinical data.<sup>4</sup> For the ADAM model, a “bottom-up” approach was used in which the cumulative absorption across gastrointestinal segments was predicted based on the pH solubility and dissolution profile predicted from *in vitro* data (solubility, permeability, Fasted and Fed State Simulated Intestinal Fluid (FaSSIF and FeSSIF), particle size, etc.). The human jejunum effective permeability ( $P_{eff, man}$ ) was predicted from heterogeneous human epithelial colorectal adenocarcinoma cells (Caco-2) data (**Table S3**). The unbound fraction in the gut ( $f_{u, gut}$ ) was assumed to be 1.

Distribution. The  $V_{ss}$  was predicted using tissue composition equations<sup>32</sup> with *in vitro* data (octanol–water partition coefficient, logP, acid dissociation constant, pKa,  $f_{u,p}$ ; **Table 1**). To capture the multiphasic plasma concentration-time profile of ITZ, the Simcyp minimal PBPK (which treats all organs other than the intestine and liver as a single compartment<sup>33</sup> plus a single adjusting compartment (SAC)) distribution model was selected. The final values of the apparent volume of SAC ( $V_{sac}$ ), the rate constant from systemic compartment to SAC ( $K_{in}$ ), and the rate constant from SAC compartment to the systemic compartment ( $K_{out}$ ) were determined based on simulations that best described the shape of observed ITZ intravenous PK profile<sup>10</sup> (**Figure S1**).

**CL.** *In vitro* enzyme kinetic parameters (maximum rate of reaction ( $V_{max}$ ) and unbound concentration of substrate to achieve half  $V_{max}$  ( $K_{m,u}$ )) determined by the WG were incorporated into the model and assigned to CYP3A4 mediated metabolism (**Table 1**).

**CYP3A4 inhibition by ITZ.** The  $K_{i,u}$  for ITZ calculated from the half maximal inhibitory unbound concentration ( $IC_{50,u}$ ) generated using MDZ as a substrate in human liver microsomes by the WG was input into the model (**Table 1**).

**PBPK model for OH-ITZ Formation.** The elimination of ITZ is predominantly via CYP3A4-mediated metabolism to form OH-ITZ.<sup>10,34,35</sup> Therefore, the CL of ITZ served as the formation CL of OH-ITZ in the model.

**Distribution.** The  $V_{ss}$  for OH-ITZ was predicted with *in vitro* data as described for ITZ (**Table 1**). The Simcyp minimal distribution model with a SAC was used to capture the shape of OH-ITZ concentration-time profile after intravenous administration of ITZ.

**CL.** *In vitro*  $V_{max}$  and  $K_{m,u}$  values determined by the WG were used to parameterize the CL of OH-ITZ and were assigned to CYP3A4 (**Table 1**).

**CYP3A4 inhibition by OH-ITZ.** The  $K_{i,u}$  for OH-ITZ calculated from the  $IC_{50,u}$  generated using MDZ as a substrate in human liver microsomes by the WG was input into the model (**Table 1**).

#### PBPK model verification

**Verification of PBPK model for ITZ and OH-ITZ PK predictions.** The performance of the PBPK model was verified using PK data from the WG. In addition to the mean

Table 1 PBPK Model Input Parameters for ITZ and OH-ITZ

Parameter	Itraconazole (ITZ)		OH-Itraconazole (OH-ITZ)	
	Value	References/comments	Value	References/comments
MW (g/mol)	705.6		721.7	
logP <sub>o,w</sub>	4.9	WG	4.1	WG
Compound type	Monoprotic base		Mono-base	
pKa1	3.64	WG	4.0	WG
B/P	0.6	WG	0.55	WG
f <sub>u,p</sub>	0.0015	Di et al. 2017 <sup>38</sup> ; see Discussion section for details	0.012	Extrapolated, see Discussion section for details
First-order absorption model				
Fa	0.7/0.5/0.6	Solution fasted/capsule fasted/ capsule fed <sup>a</sup>		
ka (hour <sup>-1</sup> )	0.45/0.2/0.25			
f <sub>u,gut</sub>	1	Assumed	1	Assumed
Q <sub>gut</sub> (L/hour)	13.7	Simcyp predicted		
Caco-2 P <sub>app</sub> (10 <sup>-6</sup> cm/second)	2.5	WG		
Pe <sub>ff</sub> (10 <sup>-4</sup> cm/second)	3.75	Predicted with scalar of 14.1		
ADAM absorption model (for capsule fasted/fed)	IR			
Intrinsic solubility (mg/mL)	0.15	pH 1.1, Taupitz 2013 <sup>42</sup>		
FaSSIF/FeSSIF	0.007/0.005	WG		
Caco-2 P <sub>app</sub> (10 <sup>-6</sup> cm/second)	2.5	WG		
Pe <sub>ff</sub> (10 <sup>-4</sup> cm/second)	1.3	Predicted with scalar of 4.57		
Dissolution	Predicted	Diffusion layer model		
Particle size (μm)	3			
Density (g/mL)	1.2			
Minimal + SAC PBPK distribution model				
V <sub>ss</sub> (L/kg)	4.75	Simcyp predicted, method 1	4.72	Simcyp predicted, method 1
V <sub>sac</sub> (L/kg)	3	Best fit <sup>a</sup>	2.5	Best fit <sup>a</sup>
K <sub>in</sub> /K <sub>out</sub> (1/hour)	0.2/0.1	Best fit <sup>a</sup>	0.005/0	Best fit <sup>a</sup>
Elimination				
V <sub>max</sub> (CYP3A4) pmol/minute/mg protein	44.5	WG	23	WG
K <sub>m,u</sub> (CYP3A4) (μM)	0.0233	WG	0.0399	WG
CL <sub>R</sub> (L/hour)	0		0	
Active uptake into hepatocyte	3.5	Estimated to best describe ITZ IV CL <sup>a</sup>	-	
CYP inhibition				
K <sub>i,u</sub> (μM) on CYP3A4	0.0010	WG, microsomes	0.0082	WG, microsomes

ADAM, advanced dissolution, absorption, and metabolism; B/P ratio, blood/plasma partition ratio; Caco-2, heterogeneous human epithelial colorectal adenocarcinoma cells; CL, clearance; CLR, renal clearance; CYP, cytochrome P450; CYP3A, cytochrome P450 3A; fa, fraction absorbed (three different values correspond to three different formulation/food states, for a given formulation/food state, the same fa is used in the model simulation regardless of the dose levels); FaSSIF, Fasted State Simulated Intestinal Fluid; FeSSIF, Fed State Simulated Intestinal Fluid; f<sub>u,p</sub>, free fraction in plasma; f<sub>u,gut</sub>, free fraction in gut enterocyte; IR, immediate release; ITZ, itraconazole; IV, intravenous; ka, absorption rate constant; K<sub>i,u</sub>, unbound concentration of IC50/2; k<sub>in</sub>, rate constant from systemic compartment to SAC; K<sub>m,u</sub>, unbound concentration of substrate to achieve half V<sub>max</sub>; k<sub>out</sub>, rate constant from SAC compartment to the systemic compartment; logP<sub>o,w</sub>, calculated octanol-water partition coefficient; MW, molecular weight; OH-ITZ, hydroxyitraconazole; P<sub>app</sub>, apparent permeability; PBPK, physiologically-based pharmacokinetic; Pe<sub>ff</sub>, effective permeability; pKa, acid dissociation constant; Q<sub>gut</sub>, nominal flow through the gut; SAC, single adjusting compartment; V<sub>max</sub>, maximum rate of reaction; V<sub>sac</sub>, volume of the single adjusted compartment; V<sub>ss</sub>, volume of distribution at steady state; WG, working group, these parameters are from *in vitro* measurements by working group companies.

<sup>a</sup>These parameters were adjusted or estimated to best fit to the observed data.

plasma-concentration time profiles, information on dosage form, dose regimen, and fed status were available for all studies used in the model verification, whereas age, gender, and body weight information were only available for some data sets. Of 17 clinical studies, 16 were selected for model verification based on whether sufficient data were available (Table S1).

The simulations were performed using 10 virtual trials of 10 healthy volunteers aged 20–50 years and a 1:1

female-to-male ratio. For ITZ-solution PK studies, the first-order absorption model was used, and for the capsule, both the first-order and ADAM models were used. The dose regimens in the virtual trials were identical to those used in the clinical studies. Agreement between the simulated and observed ITZ and OH-ITZ PK profiles was evaluated by overlaying the simulated mean concentration-time profiles with mean clinical data.

### Verification of the PBPK model for ITZ DDI predictions.

Verification of the model to predict the magnitude of DDI between ITZ and seven CYP3A4 substrates (MDZ, paroxetine, quinidine, repaglinide, simvastatin, triazolam, and zolpidem) was performed by simulating DDIs from 20 reported clinical studies. The Healthy Volunteers Population in Simcyp was used with 10 trials and 10 subjects per trial. The simulated age range and fraction of female subjects were as reported for each clinical trial. If the fraction of females was not reported, a value of 0.5 was assigned. For a few clinical studies, there was limited dosing information. If there was no mention of dose staggering, it was assumed that the victim drug was dosed simultaneously with ITZ. When dosing in the fed or fasted state was not mentioned, the fasted state was assumed. The default Simcyp compound files for the seven CYP3A4 substrates were used.<sup>7,36</sup> Descriptions of the simulated trials are provided in **Table S2**.

For each clinical trial, the area under the concentration-time curve (AUC) and maximum plasma concentration ( $C_{max}$ ) ratios were reported as arithmetic means or geometric mean ratios. The percent prediction error (PE) was calculated for the AUC and  $C_{max}$  ratios as shown in Eq.1. The guest criteria were then followed to assess model predictability.<sup>37</sup>

$$\text{Prediction error (PE)} = \frac{\text{Predicted value} - \text{Observed value}}{\text{Observed value}} \times 100 \quad (1)$$

### ITZ clinical DDI study design

The PBPK model was used to simulate various clinical scenarios to verify the IQ CPLG recommendations or to recommend an alternative optimal DDI study design. Oral MDZ (2 mg) was used as a probe CYP3A4 substrate with ITZ administered as a solution in the fasted state or a capsule in the fed state. The various simulated clinical study design scenarios including those previously recommended by the IQ CPLG<sup>3</sup> are illustrated in **Figure 2** and detailed as follows:

1. Impact of total duration (4, 6, or 8 days) of 200 mg once daily (q.d.) ITZ administration (MDZ administered on day 4).
2. Impact of substrate administration on different days (days 4, 6, or 8) with ITZ administration for 14 days. The different dose regimens of ITZ simulated were (i) 200 mg q.d.; (ii) 200 mg twice daily (b.i.d.) loading dose on day 1, 200 mg q.d. thereafter; (iii) 200 mg b.i.d. on day 1 and 100 mg b.i.d. thereafter; (d) 400 mg q.d. on day 1 and 200 mg q.d. thereafter.
3. Impact of timing of MDZ administered on day 4, either simultaneously or 1, 2, or 3 hours post-ITZ dosing, 200 mg q.d. for 4, 6, or 8 days (0, 2, or 4 days post-MDZ dose).

Lastly, the impact of substrate half-life was evaluated. The MDZ compound file was modified to create a hypothetical range of half-lives by varying  $V_{ss}$ , with all other parameters unchanged.

## RESULTS

### Data collection—in vitro data

Physicochemical properties for ITZ and its metabolites generated by the WG are summarized in **Table S3**. The *in vitro* binding data, enzyme kinetics, and CYP3A4 inhibition data for ITZ and its metabolites generated by the WG in comparison with the literature data are summarized in **Table S4**.

### PBPK models for ITZ and OH-ITZ

The contribution of each circulating metabolite to the total inhibition was estimated based on *in vitro* and clinical data generated by the WG. The mean unbound plasma concentration-time data for ITZ and three metabolites from four studies (ITZ solution 200 mg q.d.) were plotted and compared with the unbound *in vitro* CYP3A4  $K_i$  values (**Figure S3**). These data show unbound plasma concentrations of ITZ and OH-ITZ are above the unbound CYP3A4  $K_i$  values up to approximately 5 hours and 12 hours, respectively, after

Study Design for Clinical Scenarios Simulated using ITZ and OH-ITZ PBPK Models

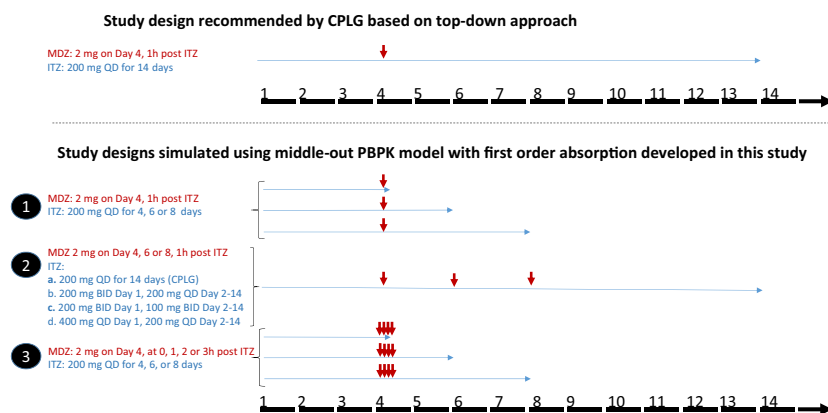


**Figure 2** Study design for clinical scenarios simulated using itraconazole (ITZ) and hydroxyitraconazole (OH-ITZ) physiologically-based pharmacokinetic (PBPK) models. CPLG, Clinical Pharmacology Leadership Group; b.i.d., twice a day; MDZ, midazolam; q.d., once a day.

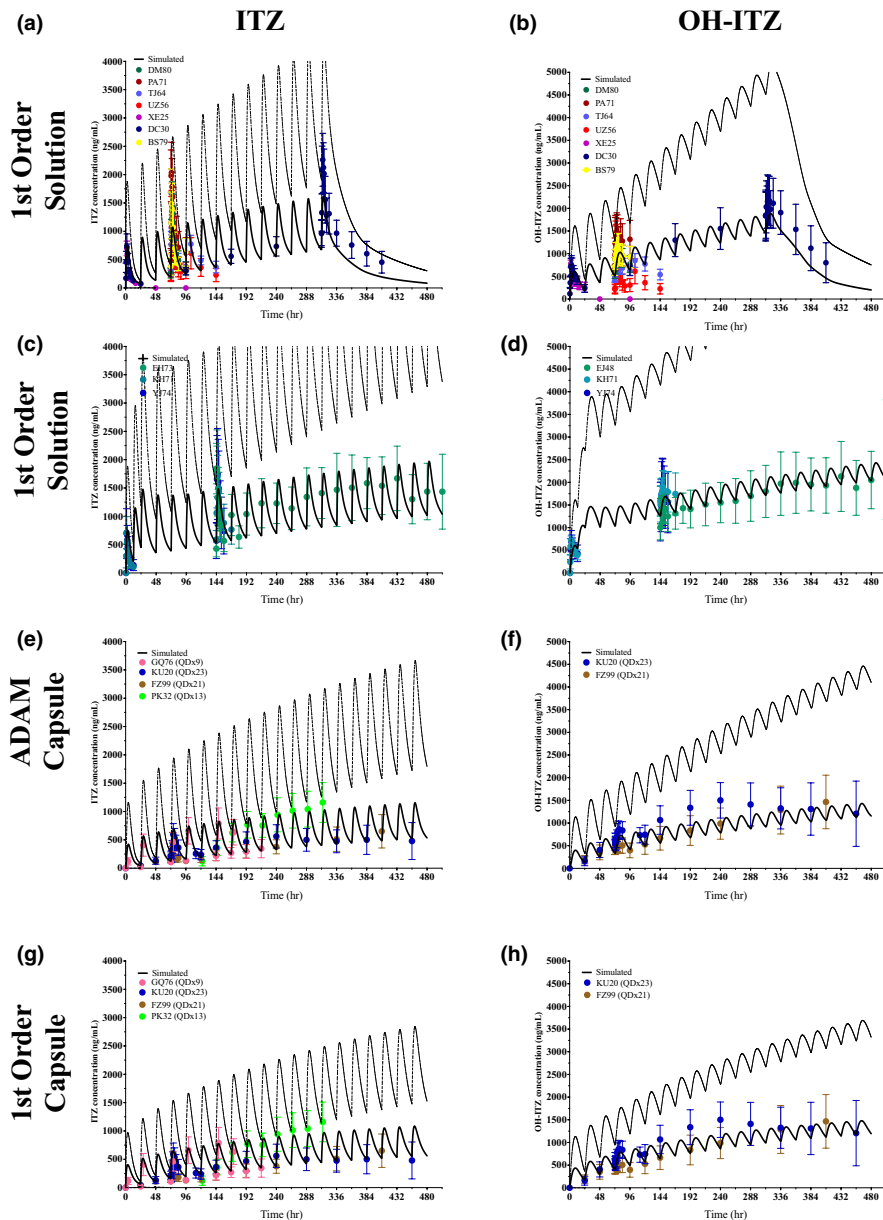


**Figure 3** Physiologically-based pharmacokinetic (PBPK) model simulated vs. observed itraconazole (ITZ) and hydroxyitraconazole (OH-ITZ) plasma concentration–time profiles. **(a, b)** Simulated (by first-order absorption model) and observed ITZ and OH-ITZ PK profiles after multiple doses of 200 mg once daily ITZ solution under fasted conditions. Observed data are from seven different studies. **(c, d)** Simulated (by first-order absorption model) and observed ITZ and OH-ITZ PK profiles after 200 mg twice a day on day 1 followed by 200 mg once-daily (q.d.) dosing of ITZ solution under fasted conditions. Observed data are from three different studies. **(e, f)** Simulated (by ADAM absorption model) and observed ITZ and OH-ITZ PK profiles after 200 mg q.d. dosing of ITZ capsules under fasted and fed conditions. Observed data are from four different studies, two of which had OH-ITZ concentration measurements. **(h, i)** Simulated (by first-order absorption model) and observed ITZ and OH-ITZ PK profiles after 200 mg q.d. dosing of ITZ capsules under fed conditions. Observed data are from four different studies, two of which reported OH-ITZ concentrations. For all panels, black lines represent the simulated mean concentration and the dotted lines represent standard derivation of 100 individuals (10 trials of 10 subjects per trial) simulated. The clinical study numbers correspond to the study descriptions in **Table S1**. ADAM, advanced dissolution, absorption, and metabolism.

dosing on day 4, whereas the unbound plasma concentrations for keto-ITZ and ND-ITZ are approximately 10-fold to 20-fold lower than the unbound *in vitro*  $K_i$  values. This suggests that keto-ITZ and ND-ITZ are unlikely to contribute to the inhibition of CYP3A4. Therefore, the developed PBPK model was restricted to ITZ and OH-ITZ.

The model input parameters are shown in **Table 1**. The  $V_{ss}$  was predicted to be 4.75 L/kg for ITZ and 4.72 L/kg for OH-ITZ. In comparison to the full PBPK distribution model, the minimal distribution model more appropriately described the shape of the concentration-time profile for both ITZ and OH-ITZ. The elimination of ITZ and OH-ITZ was parameterized

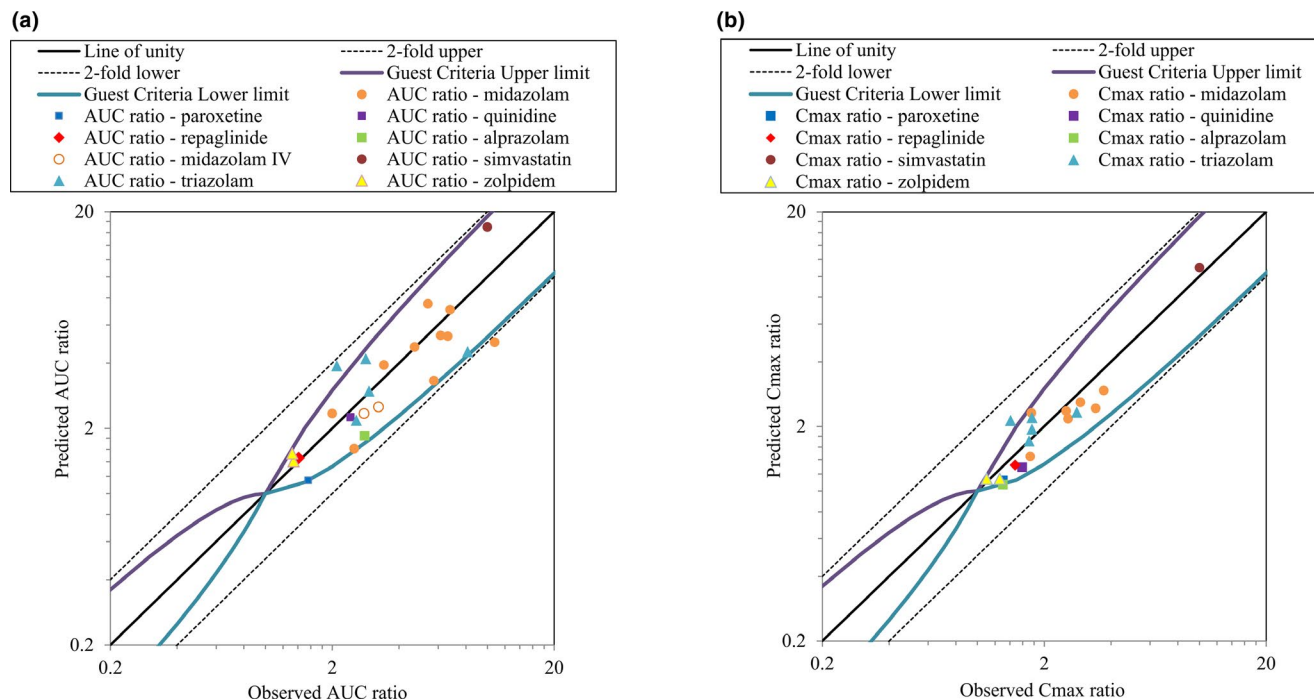


**Figure 4** Observed vs. predicted AUC ratio (a) and C<sub>max</sub> ratio (b) of CYP3A substrates in the presence and absence of ITZ. AUC, area under the concentration-time curve; C<sub>max</sub>, maximum plasma concentration; CYP3A, cytochrome P450 3A; i.v., intravenous.

with *in vitro* CYP3A4 enzyme kinetic parameters. The  $K_{m,u}$  and  $V_{max}$  were 0.0233  $\mu$ M and 44.5 pmol/minute/mg protein for ITZ and 0.0399  $\mu$ M and 23.0 pmol/minute/mg protein for OH-ITZ, respectively. For ITZ, the *in vitro* metabolism data underpredicted the *in vivo* CL of ITZ (~9 L/hour predicted, ~21 L/hour observed at 100 mg i.v. dose).<sup>10,35</sup> One hypothesis to explain the higher *in vivo* ITZ CL is the contribution of hepatic uptake of ITZ through transporters because both *in vitro* human hepatic uptake experiments and preclinical *in vivo* data suggest that ITZ is a substrate for hepatic uptake transporters (details in the **Supplemental Material**). To account for this, a scaling factor of 3.5 was incorporated into the model to recover the observed CL. The resulting model captured the observed PK profile of ITZ and the formation of OH-ITZ after intravenous administration of 50, 100, 200, and 300 mg ITZ (**Figure S1**).

For the first-order absorption model, the  $f_a$  and  $k_a$  for the ITZ solution (fasted) and capsule (fasted and fed) obtained using a top-down approach<sup>4</sup> are listed in **Table 1**. The ADAM absorption model underpredicted the observed ITZ exposure. An increase of the  $P_{eff,man}$  predicted based on the measured permeability data was needed to capture the observed data. To describe the food effect of ITZ dosed as a capsule, the fed-state gastric emptying time was adjusted from 1 to 2.1 hours. The final parameters for the ADAM model, built using a middle-out approach, are listed in **Table 1**, and the simulated ITZ and OH-ITZ PK profiles from the orally dosed ITZ capsule in the fed state are presented in **Figure S2**.

#### PBPK model verification

**Verification of the PBPK model for ITZ and OH-ITZ PK prediction.** The ability of the model to predict ITZ and OH-ITZ PK was evaluated against 16 multiple-dose

ITZ PK studies that were not used in model development (**Table S1**). The simulated vs. observed PK profiles are presented in **Figure 3** and **Figure S4**. Overall, the simulations captured the observed data for both solution and capsule ITZ studies under the fasted and fed states. In general, the accumulation of ITZ and OH-ITZ concentrations over time were reasonably described by the model, with accumulation ratios of ~2-fold for ITZ and ~3.5-fold for OH-ITZ after 200 mg q.d. or 200 mg b.i.d. on day 1 followed by 200 mg q.d. of ITZ in solution (fasted) or capsule (fed). Little difference was observed between the first-order and ADAM absorption models for the capsule administered under fed conditions (**Figure 3e,f,h,i**). The clinical studies differed in their study design and time of blood sampling, so head-to-head C<sub>max</sub> and AUC comparisons were not conducted.

#### Verification of the PBPK model for ITZ DDI prediction.

The predicted ITZ and OH-ITZ PK profiles are comparable between the first-order and ADAM absorption models, therefore, in view of some limitations in simulating DDIs with the current ADAM model (see **Supplementary Material**), the first-order absorption model was used to simulate DDIs. The overall performance of the current ITZ and OH-ITZ PBPK models for predicting CYP3A4-mediated DDIs between ITZ and seven substrates with various fraction metabolized by CYP3A ( $f_{m,CYP3A}$ ) values was found to be acceptable (**Table S5**). Of the 24 observed and predicted AUC ratios, 22 (92%) were within or at the guest criteria, with only one trial at or below the twofold boundary. Of the 19 observed and predicted C<sub>max</sub> ratios, 18 (95%) were within or at the guest criteria limit, with no simulated DDI beyond the twofold boundary (**Figure 4**). In addition, the

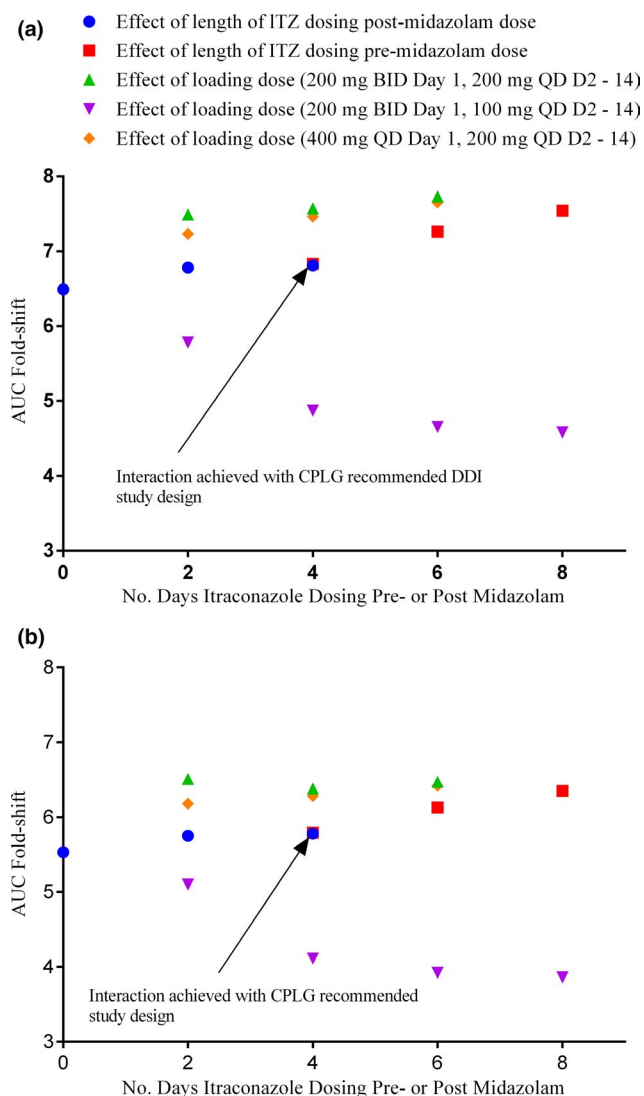


**Figure 5** Effect of length of itraconazole (ITZ) dosing and administration of a loading dose on the predicted AUC ratio of midazolam (MDZ). (a) Plot for ITZ dosed as a solution in the fed state. (b) Plot for ITZ dosed as capsule in the fasted state. The effect of length of ITZ dosing post-MDZ dose corresponds to **Figure 2, part 1**. The effect of length of ITZ dosing pre-MDZ dose and effect of a loading dose correspond to **Figure 2, part 2a–2c**. b.i.d., twice a day; CPLG, Clinical Pharmacology Leadership Group; DDI, drug–drug interaction; q.d., once a day.

percent error of the predicted AUC ratios from the two ITZ and intravenous MDZ DDI studies were relatively low at –16% and –22%, respectively, suggesting good model performance in predicting hepatic CYP3A4-mediated DDIs.

#### Recommendation of ITZ clinical DDI study design

The results of the simulations with different study designs are presented in **Figures 5 and 6**. As expected, a longer duration of ITZ dosing preadministration and postadministration of MDZ led to a greater magnitude of DDI. Higher AUC ratios were seen when a loading dose of ITZ (200 mg b.i.d. or 400 mg q.d.) was given on day 1, followed by a

200 mg dose q.d. thereafter. In addition, higher AUC ratios were seen for the ITZ solution (fasted; **Figure 5a**) when compared with the capsule (fed; **Figure 5b**). However, the trends with respect to the number of days of ITZ dosing prior to MDZ, duration of administration, and loading dose are similar between the capsule (fed) and solution (fasted) (**Figure 5a,b**). Although the simulations of dose staggering showed that a slightly higher DDI ratio was obtained for the solution (fasted) when MDZ was simultaneously dosed with ITZ and for the capsule (fed) when MDZ was dosed 1 hour after administration of ITZ, the difference was not significant in either case (**Figure 6**). For both formulations, the maximal inhibitory effect declined if MDZ was dosed 2 hours after ITZ administration. Finally, the simulations of ITZ interaction with a hypothetical substrate indicated that continuing ITZ dosing for 4–5 substrate half-life post-substrate administration is necessary to reach maximal interaction (**Figure S5**).

## DISCUSSION

### *In vitro* data

ITZ is highly lipophilic, making an accurate measurement of  $f_{u,p}$  a challenge. In a recent independent IQ effort, a mean  $f_{u,p}$  value of 0.0015 for ITZ was reported (generated across 11 companies).<sup>38</sup> Considering that this is the most recent large data set obtained, this value was selected for our model. In both the WG ( $f_{u,p}$  ITZ-0.001 and OH-ITZ-0.0084) and previously published ( $f_{u,p}$  ITZ-0.002 and OH-ITZ-0.017<sup>39</sup>) data sets, the OH-ITZ  $f_{u,p}$  was approximately eightfold greater than ITZ. Therefore, we used  $f_{u,p} = 0.012$  ( $0.0015 \times 8$ ) for OH-ITZ, which was in the range of the previously reported value and the data generated by the WG.

The  $f_{u,mic}$  of ITZ determined by the WG was similar to values reported in the literature. However, all three metabolites were found to have higher  $f_{u,mic}$  values than previously reported,<sup>34</sup> with ND-ITZ showing the largest difference (0.026 at 0.025 mg/mL using tube adsorption method vs. 0.70 obtained by the WG using equilibrium dialysis). The  $f_{u,mic}$  generated by the WG brings the value up to the same range as the other ITZ metabolites, which is expected based on their similar physicochemical properties (**Table S3**).

Our analysis using the *in vitro* data (CYP3A4  $K_i$ ,  $f_{u,mic}$ , and  $f_{u,p}$ ) and clinical PK data confirms the significant contributions of ITZ and OH-ITZ on the inhibition of CYP3A4 and low likelihood of significant contributions from keto-ITZ and ND-ITZ. Our findings are generally consistent with the minimal role of keto-ITZ reported by Templeton *et al.*<sup>17</sup> However, for ND-ITZ, Templeton *et al.* reported an estimated 30–40% contribution to the total CYP3A4 inhibition.<sup>17,40</sup> This discrepancy was traced to the  $f_{u,mic}$  used to correct the ND-ITZ  $K_i$ , as described previously. Taken together with the apparent  $K_i$  obtained in microsomes, ND-ITZ was approximately 40-fold less potent than previously reported (**Table S4**). Assuming unbound liver concentrations of keto-ITZ and ND-ITZ are not markedly greater than unbound plasma concentrations, this suggests that neither metabolite likely contributes significantly to the inhibitory effects following ITZ administration.

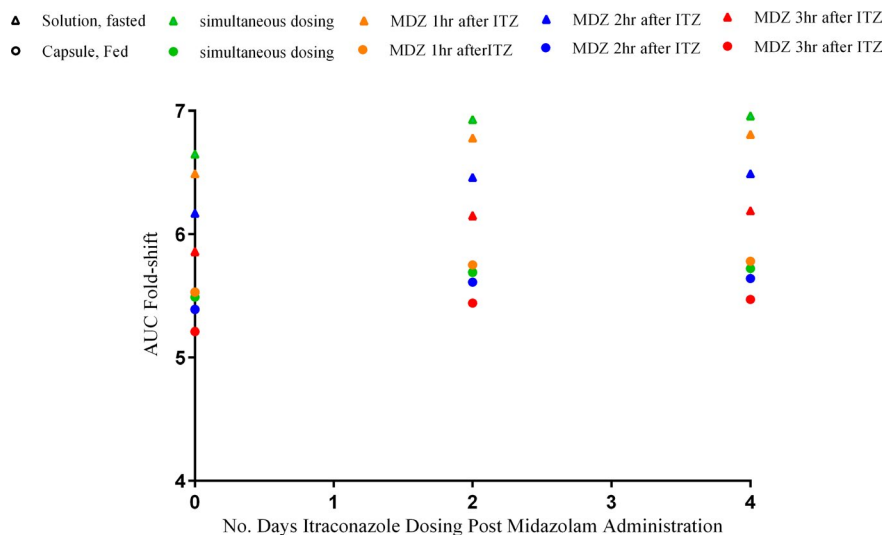


**Figure 6** Effect of timing of midazolam (MDZ) dose with respect to itraconazole (ITZ) on predicted area under the concentration-time curve (AUC) ratio of MDZ (corresponding to study design in **Figure 2, part 3**).

### ITZ and OH-ITZ PBPK models

The PBPK model was built using the newly generated *in vitro* data and verified using 16 sets of clinical data provided by the WG. Although the bottom-up approach was used for model development, the adjustment of some parameters was necessary to best describe the observed data. The minimal distribution model was employed to accurately capture the shape of ITZ and OH-ITZ PK curve. Although further characterization of the full distribution model in describing ITZ and OH-ITZ PK shape is of great interest, the minimal distribution model used in our PBPK model was considered adequate for simulating ITZ DDI that mainly happen in the liver and intestine during first-pass metabolism. Nevertheless, when compared with the existing models, the current work provides a greater mechanistic understanding of ITZ PK and DDI characteristics. Comparisons of model parameters and DDI predictions between the WG model and the Simcyp model are provided in the **Supplementary Material**.

To appropriately describe the significant accumulation, robust measurements of  $K_m$ ,  $V_{max}$ , CYP3A4  $K_i$ ,  $f_{u,p}$ , and  $f_{u,mic}$  for ITZ and OH-ITZ were obtained by the WG. To understand the underprediction of ITZ CL from *in vitro* enzyme kinetic data, different causes including higher  $V_{max}$  and lower  $K_{m,u}$  *in vivo* as well as active hepatic uptake of ITZ were hypothesized. Hepatic uptake was incorporated into the model based on the totality of *in vitro* human hepatocyte and *in vivo* preclinical evidence. However, studies to further understand the mechanism of hepatic uptake and the use of quantitative transporter kinetic data to describe this process were not explored in current study. To understand the impact of the CYP3A4  $K_i$  on the accumulation after repeat dosing, sensitivity analyses were conducted with the  $K_i$  determined from various sources, including the  $K_i$  determined by the WG in microsomes with MDZ and testosterone as substrates and the  $K_i$  determined in hepatocytes in the presence of plasma with MDZ as a substrate.<sup>41</sup> Although all of the above enabled

the model to predict significant accumulations of ITZ and OH-ITZ, the simulation using the  $K_i$  value obtained from the  $IC_{50}$  measurements in microsomes with MDZ as a substrate ( $n = 4$  determined by the WG) best described the accumulation of ITZ and OH-ITZ based on the clinical data used for the model development. Although the model has been verified with existing clinical data for the prediction of ITZ and OH-ITZ accumulation under commonly used clinical dose regimens (e.g., 200 mg once daily dose or one twice daily loading dose followed by once daily dosing), additional verification of the model to describe twice daily dosing for multiple days is necessary once more clinical data become available.

The performance of the ADAM absorption model built using a middle-out approach is comparable with the first-order absorption model in terms of predicting human PK. The initial attempt of using a mechanistic absorption model to predict ITZ DDI is based on the hypothesis that a more accurate prediction of DDI in the gut could be achieved when the gut enterocyte concentration, instead of the portal vein concentration, is used as the interacting concentration, as structured in ADAM model. However, this will only happen (the gut enterocyte concentration as the interacting concentration) in Simcyp when both the substrate and inhibitor (ITZ) are modeled with ADAM absorption. Because very few substrates with validated ADAM models are available in Simcyp, the benefit of the mechanistic absorption modeling of ITZ as an inhibitor is not apparent when the substrates are modeled with first-order absorption. In addition, the simulations using ITZ with first-order and ADAM absorption models indicated that as long as the simulated plasma concentrations are comparable, the simulated DDI using portal vein concentration as interacting concentration is very comparable between the two absorption models (**Figure S6**). Therefore, DDI simulations using ITZ with the ADAM model was deemed unnecessary, especially considering the longer simulation times required. Furthermore, the food effect on inhibitors

with the ADAM model cannot be simulated in Simcyp V16 (**Supplementary Material**).

**ITZ DDI predictions.** Using the guest criteria (**Figure 4**), 22 trials (of 24) were predicted within or at the limit. Considering the complexity and variability of the ITZ clinical data<sup>35</sup> used in the model verification, the performance of the PBPK model developed is considered acceptable for prospective ITZ DDI risk assessment for new chemical entities as CYP3A substrates. However, the estimation of  $f_{m,CYP3A}$  in the liver and gut wall for a new chemical entity using retrospective simulations by the PBPK model may require sensitivity analysis on key determinants of the parameters.

**ITZ DDI study design.** In general, the DDI simulations from the PBPK model developed in this work largely confirmed the study design proposed by the IQ CPLG.<sup>3</sup> The simulation results support the following recommendations for an improved study design of ITZ DDI.

1. Longer administration of ITZ (>3 days, closer to the steady state) prior to MDZ dosing increased the inhibitory effects but should be balanced with the total duration of the ITZ administration (approximately 14 days) by considering the half-life of the substrate, especially for the long half-life substrates. The CPLG recommended a run-in period (3 days) provided reasonable inhibitory effects.
2. A loading dose of 200 mg b.i.d. or 400 mg q.d. on day 1 showed the highest inhibitory effects; however, it should be used with caution for safety reasons. This approach could be useful for long half-life victim compounds, when the coverage of ITZ is needed for 4–5 half-lives of the substrate and the total dosing time of ITZ is limited to approximately 14 days.
3. Our study shows that the dose staggering of MDZ and ITZ (simultaneous vs. 1 hour after) has no significant impact on ITZ DDI, which could provide a practical advantage beyond that recommended by the CPLG.
4. A sensitivity analysis of the substrate half-life confirmed the recommendation from the CPLG<sup>3</sup> about covering 4–5 half-lives post-substrate administration to reach maximal interaction.

**Supporting Information.** Supplementary information accompanies this paper on the *CPT: Pharmacometrics & Systems Pharmacology* website ([www.psp-journal.com](http://www.psp-journal.com)).

**Figure S1.** Simulated vs. observed itraconazole (ITZ) and hydroxy-itraconazole (OH-ITZ) pharmacokinetic (PK) profiles from intravenous-dosed (50–300 mg) ITZ studies.

**Figure S2.** Simulated vs. observed ITZ (a) and OH-ITZ (b) PK profiles from an orally dosed 200 mg ITZ capsule under fed conditions; simulation using the advanced dissolution, absorption, and metabolism (ADAM) absorption model.

**Figure S3.** Unbound plasma concentrations of (a) ITZ, (b) OH-ITZ, (c) keto-itraconazole (keto-ITZ), (d) N-desmethyiltraconazole (ND-ITZ) on

day 4 following 200 mg once-a-day administration of ITZ oral solution ( $n = 3–5$  studies).

**Figure S4.** Simulated vs. observed ITZ and OH-ITZ PK profiles for less common ITZ dose regimens.

**Figure S5.** Effect of substrate half-life on ITZ dosing requirements.

**Figure S6.** Simulated drug–drug interactions (DDIs) using physiologically-based pharmacokinetic (PBPK) models with either first-order or ADAM absorption models.

#### Supplementary Methods and Supplementary Tables.

**Table S1.** Clinical data collected from the working group (WG) member companies and literature.

**Table S2.** Itraconazole DDI trials used in PBPK model verification.

**Table S3.** Physicochemical parameters generated by the WG member companies.

**Table S4.** *In vitro* binding data, enzyme kinetics, and inhibition for ITZ and metabolites.

**Table S5.** PBPK model predicted vs. observed area under the concentration-time curve (AUC) and maximum plasma concentration ( $C_{max}$ ) ratios of substrates in the presence and absence of ITZ.

**Table S6.** Comparison of PBPK input parameters for ITZ and OH-ITZ in the WG model and in the Simcyp (latest) model.

#### PBPK compound files.

**Acknowledgments.** The authors thank Mohamad Shebley (Abbvie), Kenneth Anderson and Cynthia Chavez-Eng (Merck Sharp & Dohme Corp., a subsidiary of Merck & Co., Inc., Kenilworth, NJ), Fang Ma (Genentech), Christian Lüpfer (Merck KGaA), Shinji Iwasaki (Takeda), Manthena Varma (Pfizer), Emi Kimoto (Pfizer), Anil Koulur (Lilly), Helen Gu and Donald Chun (Novartis) and Luc Rougee (Lilly) for their contributions to the *in vitro* and *in vivo* data collection and/or model simulations or valuable discussion.

**Funding.** No funding was received for this work.

**Conflict of Interest.** The authors declared no competing interests for this work.

**Author Contributions.** Y.C., T.D.C., E.C., H.E., L.L., N.P., S.A.P., E.S., P.S., H.T., V.V.U., M.Z., A.Z.X.Z., and S.D.H. wrote the manuscript. Y.C., T.D.C., E.C., H.E., L.L., N.P., S.A.P., E.S., P.S., H.T., V.V.U., M.Z., A.Z.X.Z., and S.D.H. designed the research. Y.C., T.D.C., E.C., H.E., L.L., N.P., S.A.P., E.S., P.S., H.T., V.V.U., M.Z., A.Z.X.Z., and S.D.H. performed the research. Y.C., T.D.C., E.C., H.E., L.L., N.P., S.A.P., E.S., P.S., H.T., V.V.U., M.Z., A.Z.X.Z., and S.D.H. analyzed the data.

1. European Medicines Agency recommends suspension of marketing authorisations for oral ketoconazole. Benefit of oral ketoconazole does not outweigh risk of liver injury in fungal infections. EMA/458028/2013. (2013). <[https://www.ema.europa.eu/en/documents/press-release/european-medicines-agency-recommendssuspension-marketing-authorisations-oral-ketoconazole\\_en.pdf](https://www.ema.europa.eu/en/documents/press-release/european-medicines-agency-recommendssuspension-marketing-authorisations-oral-ketoconazole_en.pdf)>.
2. FDA Drug Safety Communication: FDA limits usage of Nizoral (ketoconazole) oral tablets due to potentially fatal liver injury and risk of drug interactions and adrenal gland problems. UCM 362444. (2013). UCM. <<https://www.fda.gov/drugs/drug-safety-and-availability/fda-drug-safety-communication-fda-limits-usagenizoral-ketoconazole-oral-tablets-due-potentially>>.
3. Liu, L. *et al.* Best practices for the use of itraconazole as a replacement for ketoconazole in drug–drug interaction studies. *J. Clin. Pharmacol.* **56**, 143–151 (2016).
4. Chen, Y. *et al.* Development of a physiologically based pharmacokinetic model for itraconazole pharmacokinetics and drug–drug interaction prediction. *Clin. Pharmacokinet.* **55**, 735–749 (2016).
5. Ke, A. B., Zamek-Gliszczyński, M. J., Higgins, J. W. & Hall, S. D. Itraconazole and clarithromycin as ketoconazole alternatives for clinical CYP3A inhibition studies. *Clin. Pharmacol. Ther.* **95**, 473–476 (2014).

6. Prieto Garcia, L. *et al.* Physiologically based pharmacokinetic model of itraconazole and two of its metabolites to improve the predictions and the mechanistic understanding of CYP3A4 drug-drug interactions. *Drug Metab. Dispos.* **46**, 1420–1433 (2018).
7. Marsousi, N., Desmeules, J.A., Rudaz, S. & Daali, Y. Prediction of drug-drug interactions using physiologically-based pharmacokinetic models of CYP450 modulators included in Simcyp software. *Biopharm. Drug Dispos.* **39**, 3–17 (2018).
8. FDA Physiologically Based Pharmacokinetic Analyses—Format and Content, Guidance for Industry (2016). <<https://www.fda.gov/regulatory-information/search-fda-guidance-documents/physiologically-based-pharmacokinetic-analyses-format-and-content-guidance-industry>>.
9. European Medicines Agency. Guideline on the qualification and reporting of physiologically based pharmacokinetic (PBPK) modelling and simulation. EMA/CHMP/458101/2016. (2016). <[https://www.ema.europa.eu/en/documents/scientific-guideline/draft-guideline-qualification-reporting-physiologically-based-pharmacokinetic-pbpb-modelling\\_en.pdf](https://www.ema.europa.eu/en/documents/scientific-guideline/draft-guideline-qualification-reporting-physiologically-based-pharmacokinetic-pbpb-modelling_en.pdf)>.
10. Mouton, J.W. *et al.* Pharmacokinetics of itraconazole and hydroxyitraconazole in healthy subjects after single and multiple doses of a novel formulation. *Antimicrob. Agents Chemother.* **50**, 4096–4102 (2006).
11. Barone, J.A. *et al.* Enhanced bioavailability of itraconazole in hydroxypropyl-beta-cyclodextrin solution versus capsules in healthy volunteers. *Antimicrob. Agents Chemother.* **42**, 1862–1865 (1998).
12. Barone, J.A. *et al.* Food interaction and steady-state pharmacokinetics of itraconazole oral solution in healthy volunteers. *Pharmacotherapy* **18**, 295–301 (1998).
13. Barone, J.A. *et al.* Food interaction and steady-state pharmacokinetics of itraconazole capsules in healthy male volunteers. *Antimicrob. Agents Chemother.* **37**, 778–784 (1993).
14. Hardin, T.C. *et al.* Pharmacokinetics of itraconazole following oral administration to normal volunteers. *Antimicrob. Agents Chemother.* **32**, 1310–1313 (1988).
15. The University of Washington Drug Interaction Database (DIDB). <<https://www.druginteractioninfo.org/>>.
16. Prueksaritanont, T. *et al.* Validation of a microdose probe drug cocktail for clinical drug interaction assessments for drug transporters and CYP3A. *Clin. Pharmacol. Ther.* **101**, 519–530 (2017).
17. Templeton, I. *et al.* Accurate prediction of dose-dependent CYP3A4 inhibition by itraconazole and its metabolites from in vitro inhibition data. *Clin. Pharmacol. Ther.* **88**, 499–505 (2010).
18. Ahonen, J., Olkkola, K.T. & Neuvonen, P.J. Effect of itraconazole and terbinafine on the pharmacokinetics and pharmacodynamics of midazolam in healthy volunteers. *Br. J. Clin. Pharmacol.* **40**, 270–272 (1995).
19. Backman, J.T., Kivisto, K.T., Olkkola, K.T. & Neuvonen, P.J. The area under the plasma concentration-time curve for oral midazolam is 400-fold larger during treatment with itraconazole than with rifampicin. *Eur. J. Clin. Pharmacol.* **54**, 53–58 (1998).
20. Olkkola, K.T., Ahonen, J. & Neuvonen, P.J. The effects of the systemic antimycotics, itraconazole and fluconazole, on the pharmacokinetics and pharmacodynamics of intravenous and oral midazolam. *Anest. Analg.* **82**, 511–516 (1996).
21. Olkkola, K.T., Backman, J.T. & Neuvonen, P.J. Midazolam should be avoided in patients receiving the systemic antimycotics ketoconazole or itraconazole. *Clin. Pharmacol. Ther.* **55**, 481–485 (1994).
22. Yasui-Furukori, N. *et al.* Effect of itraconazole on pharmacokinetics of paroxetine: the role of gut transporters. *Ther. Drug Monit.* **29**, 45–48 (2007).
23. Kaukonen, K.M., Olkkola, K.T. & Neuvonen, P.J. Itraconazole increases plasma concentrations of quinidine. *Clin. Pharmacol. Ther.* **62**, 510–517 (1997).
24. Niemi, M., Backman, J.T., Neuvonen, M. & Neuvonen, P.J. Effects of gemfibrozil, itraconazole, and their combination on the pharmacokinetics and pharmacodynamics of repaglinide: potentially hazardous interaction between gemfibrozil and repaglinide. *Diabetologia* **46**, 347–351 (2003).
25. Yasui, N. *et al.* Effect of itraconazole on the single oral dose pharmacokinetics and pharmacodynamics of alprazolam. *Psychopharmacology* **139**, 269–273 (1998).
26. Yu, K.S. *et al.* Effect of the CYP3A5 genotype on the pharmacokinetics of intravenous midazolam during inhibited and induced metabolic states. *Clin. Pharmacol. Ther.* **76**, 104–112 (2004).
27. Neuvonen, P.J., Kantola, T. & Kivisto, K.T. Simvastatin but not pravastatin is very susceptible to interaction with the CYP3A4 inhibitor itraconazole. *Clin. Pharmacol. Ther.* **63**, 332–341 (1998).
28. Neuvonen, P.J., Varhe, A. & Olkkola, K.T. The effect of ingestion time interval on the interaction between itraconazole and triazolam. *Clin. Pharmacol. Ther.* **60**, 326–331 (1996).
29. Varhe, A., Olkkola, K.T. & Neuvonen, P.J. Oral triazolam is potentially hazardous to patients receiving systemic antimycotics ketoconazole or itraconazole. *Clin. Pharmacol. Ther.* **56**, 601–607 (1994).
30. Luurila, H., Kivisto, K.T. & Neuvonen, P.J. Effect of itraconazole on the pharmacokinetics and pharmacodynamics of zolpidem. *Eur. J. Clin. Pharmacol.* **54**, 163–166 (1998).
31. Greenblatt, D.J. *et al.* Kinetic and dynamic interaction study of zolpidem with ketoconazole, itraconazole, and fluconazole. *Clin. Pharmacol. Ther.* **64**, 661–671 (1998).
32. Rodgers, T. & Rowland, M. Mechanistic approaches to volume of distribution predictions: understanding the processes. *Pharm. Res.* **24**, 918–933 (2007).
33. Rowland Yeo, K., Jamei, M., Yang, J., Tucker, G.T. & Rostami-Hodjegan, A. Physiologically based mechanistic modelling to predict complex drug-drug interactions involving simultaneous competitive and time-dependent enzyme inhibition by parent compound and its metabolite in both liver and gut – the effect of diltiazem on the time-course of exposure to triazolam. *Eur. J. Pharm. Sci.* **39**, 298–309 (2010).
34. Isoherranen, N., Kunze, K.L., Allen, K.E., Nelson, W.L. & Thummel, K.E. Role of itraconazole metabolites in CYP3A4 inhibition. *Drug Metab. Dispos.* **32**, 1121–1131 (2004).
35. Heykants, J. *et al.* The clinical pharmacokinetics of itraconazole: an overview. *Mycoses* **32**(suppl. 1), 67–87 (1989).
36. Almond, L.M. *et al.* Prediction of drug-drug interactions arising from CYP3A induction using a physiologically based dynamic model. *Drug Metab. Dispos.* **44**, 821–832 (2016).
37. Guest, E.J., Aarons, L., Houston, J.B., Rostami-Hodjegan, A. & Galetin, A. Critique of the two-fold measure of prediction success for ratios: application for the assessment of drug-drug interactions. *Drug Metab. Dispos.* **39**, 170–173 (2011).
38. Di, L. *et al.* Industry perspective on contemporary protein-binding methodologies: considerations for regulatory drug-drug interaction and related guidelines on highly bound drugs. *J. Pharm. Sci.* **106**, 3442–3452 (2017).
39. Riccardi, K. *et al.* Plasma protein binding of challenging compounds. *J. Pharm. Sci.* **104**, 2627–2636 (2015).
40. Templeton, I.E. *et al.* Contribution of itraconazole metabolites to inhibition of CYP3A4 in vivo. *Clin. Pharmacol. Ther.* **83**, 77–85 (2008).
41. Mao, J., Mohutsky, M.A., Harrelson, J.P., Wrighton, S.A. & Hall, S.D. Prediction of CYP3A-mediated drug-drug interactions using human hepatocytes suspended in human plasma. *Drug Metab. Dispos.* **39**, 591–602 (2011).
42. Taupitz, T., Dressman J.B., Buchanan, C.M., Klein, S. Cyclodextrin-water soluble polymer ternary complexes enhance the solubility and dissolution behaviour of poorly soluble drugs. Case example: Itraconazole. *Eur. J. Pharm. Biopharm.* **83**, 378–387 (2013). <https://doi.org/10.1016/j.ejpb.2012.11.003>

© 2019 The Authors. *CPT: Pharmacometrics & Systems Pharmacology* published by Wiley Periodicals, Inc. on behalf of American Society for Clinical Pharmacology and Therapeutics. This is an open access article under the terms of the Creative Commons Attribution-NonCommercial License, which permits use, distribution and reproduction in any medium, provided the original work is properly cited and is not used for commercial purposes.